Journal of Scientific & Industrial Research
Vol. 82, May 2023, pp. 568-578
DOI: 10.56042/jsir.v82i05.1095

Haar Adaptive Taylor-ASSCA-DCNN: A Novel Fusion Model for Image Quality Enhancement

Vineeta Singh* & Vandana Dixit Kaushik

Department of Computer Science and Engineering, Harcourt Butler Technical University, East Campus, Nawabganj, Kanpur, Uttar Pradesh 208 002, India

Received 13 March 2022; revised 11 March 2023; accepted 12 March 2023

In medical imaging, image fusion has a prominent exposure in extracting complementary information out of varying medical image modalities. The utilization of different medical image modality had imperatively improved treatment information. Each kind of modality contains specific data regarding subject being imaged. Various techniques are devised for solving the issue of fusion, but the major issue of these techniques is key features loss in fused image, which also leads to unwanted artefacts. This paper devises an Adaptive optimization driven deep model fusing for medical images to obtain the essential information for diagnosis and research purpose. Through our proposed fusion scheme based on Haar wavelet and Adaptive Taylor ASSCA Deep CNN we have developed fusion rules to amalgamate pairs of Magnetic Resonance Imaging i.e. MRI like T1, T2. Through experimental analysis our proposed method shown for preserving edge as well as component related information moreover tumour detection efficiency has also been increased. Here, as input, two MRI images have been considered. Then Haar wavelet is adapted on both MRI images for transformation of images in low as well as high frequency sub-groups. Then, the fusion is done with correlation-based weighted model. After fusion, produced output is imposed to final fusion, which is executed through Deep Convolution Neural Network (DCNN). The Deep CNN is trained here utilizing Adaptive Taylor Atom Search Sine Cosine Algorithm (Adaptive Taylor ASSCA). Here, the Adaptive Taylor ASSCA is obtained by integrating adaptive concept in Taylor ASSCA. The highest MI of 1.672532 have been attained using db2 wavelet for image pair 1, highest PSNR 42.20993dB using db 2 wavelet for image pair 5 and lowest RMSE 5.204896 using sym 2 wavelet for image pair 5, have been shown proposed Adaptive Taylor ASO + SCA-based Deep CNN.

Keywords: Correlation-based weighted model, Deep model, Haar wavelet, Magnetic resonance imaging (MRI), Medical image fusion

Introduction

Image fusion is a prominent method utilized recently for medical diagnosis in medical field.[1] It is a strategy of mixing complementary data out of at least two modalities got from various modalities and acquiring the output image (combined picture) enhanced with data of the two modalities.[2] For gray clinical images this method has surely demonstrated its significance. Examination of edges, corners, boundaries as well as patches and so on are most significant, unavoidable and most beneficial elements of a clinical picture. Recently, medical images are extensively adapted in clinical assessment and diagnosis,[3] and thus the increasing count of images becomes easily accessible. In general, the speaking and medical imaging is splitted into functional and structural models. The structural images, like MRI offers images with anatomy data, functional image that offers functional data with less resolution. The solitary image cannot meet the clinical requirements and so integrating functional and anatomical images offer beneficial data, which tends to be very essential. The fusion of medical image is a procedure to integrate information of different images of similar position in single image that are apposite for visual perception and is needed in treatment application.[4] In majority of clinical applications; the goal of image amalgamation is to minimize the redundancy and ambiguity in final fused image whereas increasing the relative data.[5] Thus, the functional and anatomical images are integrated for inspection. Thus, the fusion is discovered as an emerging solution that aimed to combine data from several images to generate a precise definition of similar object. Medical imaging based technological models assists in treating the disease[6–8] and it helps to minimize cost of storage by minimizing the storage.

*Author for Correspondence
E-mail: cs.vineeta.singh@gmail.com

Various deep learning, machine learning and optimization and many other strategies based fusion algorithms have been proposed recently for medical diagnosis pertaining to different medical images as well as for other application areas also.[9–11] Researchers conducted a detailed analysis and review about various fusion algorithms in different domains along with medical imaging research field.[12–14]

Classical strategies are splitted in transform and spatial domains. These strategies are developed on the basis of spatial domain, which is also considered as a hotspot of the initial research. The distinctive techniques include principal assessment.[15] The common fusion techniques are splitted into four classes, like Sparse Representation (SR) techniques[16], Multi-Scale Decomposition (MSD) techniques, hybrid transform strategy. In MSD techniques, spatial-filtering and Multi-Scale Transform (MST) is extensively utilized fusion methods. The MST[17] is emerging methods due to their outstanding efficiency in mining the salient data but no single transform can entirely indicate all data of source images. In addition, some of imperative features are misplaced[18], and results in degradation of quality, like contrast decreases, ringing effect, artificial edges and colour distortion. Several fusion techniques are adapted in selecting these coefficients that is modelled through inverse transforms to establish fused image. In recent days, the sequence of frequency domain techniques are adhering with multi scale transform that involves gradient pyramid transform, Laplacian pyramid transform, Discrete Wavelet Transform (DWT), and Complex Wavelet Transform (CWT).[19]

Here principal aim is to devise an adaptive optimized deep model to amalgamate images. Here, as source images, the two MRI images have been imposed to Haar wavelet transform further generating two frequency sub-groups. Then, the fusion is performed based on correlation-based weighted model. The output produced out of fusion is further subjected to final amalgamation, which is done with DCNN. Here training of Deep CNN has been performed with devised Adaptive Taylor ASO + SCA. Here, the Adaptive Taylor ASO + SCA are developed by combining adaptive concept in Taylor ASO + SCA.

The major contribution of the presented research work involves Developed Adaptive Taylor ASO + SCA-Based Deep CNN for Multimodal Medical Image Fusion: Haar wavelet function has been used here due to its less computational cost property. Haar wavelet transform is utilized for capturing location as well as frequency related information involving temporal resolution. Here Deep CNN training has been performed with proposed Adaptive Taylor ASSCA wherein the weights of Deep CNN are tuned via proposed Adaptive Taylor ASSCA. Here, proposed Adaptive Taylor ASSCA is developed by incorporating adaptive concept in Taylor ASO + SCA.

Literature Survey

The fusion of multimodal images has gained immense popularity in medical domain as it improves the accuracy of clinical treatment and thus fuses harmonizing data. However, the acquisition of optimum value along with cost and time reduction is a major issue. The aforementioned issues along with the challenges faced, acted as an inspiration to foster an original method.

The techniques based on multimodal medical image fusion techniques are deliberated along with its merits and demerits.

Irshad & Rehman[20] devised a technique for fusing medical images with gradient compass that can effectually combine pair of medical images. Moreover, the statistical properties were utilized for adaptive pixel fusion. However, the main issue is key features loss.

To solve key feature loss issue, Jose *et al.*[21] utilized Non-Subsampled Shearlet Transform (NSST) to propose Adolescent Identity Search Algorithm (AISA) for reducing the computational cost and time related cost as well as image optimization. Here NSST involves multi-dimensional as well as multi-directional property of directional wavelet transform. Here, the boundary measure was modelled by AISA that helps to fuse image. However, the method leads to overhead.

To minimize overhead, Shehanaz *et al.*[22] proposed Optimum Weighted Average Fusion (OWAF) to amalgamate images for enhancing efficiency of multimodal mapping. Here, the classical Discrete Wavelet Transform (DWT) was utilized for decomposing multiple modalities into several subgroups. However, the method produced less accuracy.

To deal with accuracy issues, Li *et al.*[23] proposed a model for multimodal medical images amalgamation. Researchers utilized joint bilateral filter to propose two-layer decomposition strategy. The rich intensity related information involved in energy layer as well

as capturing abundant details. Moreover, a local gradient energy operator with neighbour energy and structure tensor was fused for improving the performance. However, the rich information is lost after the fusion.

He *et al.*[24] proposed a new technique incorporating benefits of Intensity Hue Saturation (IHS) as well as Principal Component Analysis (PCA) fusion algorithms for enhancing quality of images in contrast to discrete wavelet transform i.e. DWT, Brovey and PCA fusion strategies.

Bhatnagar *et al.*[25] developed a novel technique to amalgamate multimodality medical images involving non-subsampled contourlet transform i.e. NSCT.

Huang *et al.*[26] demonstrated various strategies to amalgamate medical images and different image amalgamation techniques for medical image fusion studies in latest years, and integrated the proposed fusion approaches during latest years as well as the merits of various strategies along with fusion effect.

Fusion Techniques involving deep learning strategy as well as advanced optimization strategies have demonstrated a vital role in medical field such as for cancer diagnosis, disease diagnosis, multi-modal MRI images fusion etc.

Challenges

Following challenges were encountered by classical multimodal medical image fusion strategies:

The DT-CWT method offer highest gain compared to other histogram methods. However, they failed to involve metabolic imaging, like SPECT and PET modalities. The method did not perform robustness test for attaining noise-free fusion.

For attaining noise free fusion, a two-layer decomposition method is utilized. Here, the multimodal medical images are fused and have gained popularity in the recent days, but the balance amongst the consumption of time, fusion performance and noise robustness remained a major issue.

Previously, several contrast enhancement techniques are devised for fusing the medical images, but robustness with several noises was not solved. The noise and artefacts is a major issue in functional and structural image fusion.

Proposed Scheme

The fusion of image is method, which mapped data from different image modalities in solitary image. Here, various techniques based on multimodal fusion are devised for performing the diagnosis. The Multimodal fusion helps to amalgamate the multi-modalities into a single modality image. Here image amalgamation techniques are utilized for mapping functional image into structural image for effective diagnosis. This paper devises an adaptive optimized deep model for performing the fusion of multimodal medical images involving two MRI images. Optimization strategies require setting of hyper parameter learning rate prior to training the model. In case there are not good outcomes as per this learning rate, learning rates are required to be changes as well as training the model another time. Whereas training the model is a very time consuming process in deep learning. Setting up these learning rates becomes frustrating task for researcher. Thus to solve this overhead, concept of Adaptive optimization algorithms was developed via researchers. In this, there is no need of setting learning rate again and again, here we require initiating the parameters of learning rate to 0.001 and learning rates are being updated via these adaptive optimization algorithms during training of model.

Here, the two MRI image that is MRI image-1 and MRI image-2 are imposed as an input to transform both of the image in frequency sub-groups with Haar wavelet transform. Then, the fusion of two MRI is performed using the correlation-based weighted model. The output of the initial amalgamation is then submitted to a final amalgamation accompanied via DCNN. Training of Deep CNN is performed with devised Adaptive Taylor ASO + SCA, which is developed by combining adaptive concept in Taylor ASO + SCA. Proposed work has been illustrated through Fig. 1.

Acquisition of Input MRI Images

Consider two MRI images E and F obtained from the dataset. Here two source images have been imposed to Haar wavelet transform for mining image sub-groups.

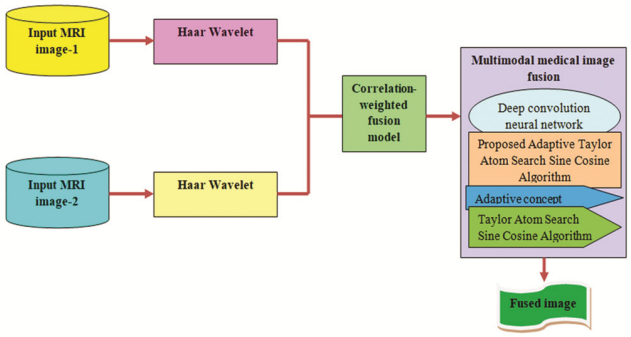

Fig. 1 — Proposed Model

Haar Transform and Generation of four sub-bands

Multiplications are not required for the Haar transform. Because there are numerous components in the Haar matrix with a value of 0, it only needs to perform additions, which cut down on computation time. It performs more quickly than the Walsh Transform, whose matrix consists of +1 as well as−1. It may be utilized to examine a signal's localized characteristic. The Haar function's orthogonal feature allows for the analysis of the input signal's frequency components. It offers a straightforward and highly effective method for analyzing a signal's local characteristics. Another discrete wavelet transform used for time resolution is the Haar transform. Haar wavelet transform is utilized for capturing location as well as frequency related information involving temporal resolution.[27] Alfred Haar devised Haar wavelet in 1909. Haar wavelet gains squared form functions in the form of wavelets. If an input is denoted via a series of 2^p numbers, using the Haar wavelet transform, additionally input values are matched, difference is stored, calculation of sum is done and repetitions is iteratively performed until and unless pairing of sums take place for finalizing next scale. At final point 2^{p-1} differences as well as final sum is calculated. The Haar wavelet transform matches the source information values, notes (preserves information about) the dissimilarities, and computes the total, that further rehashed iteratively until the aggregates combine for guaranteeing subsequent scale. Finally, 2^{p-1} contrasts and a last aggregate is inferred. The orthogonal transformation of Haar wavelet is addressed as:

$$R = SI_jS^z \quad \dots (1)$$

where, S denotes Haar transformation matrix and $(Q \times Q)$ depicts dimension of matrix, input matrix is shown via A^j while $(Q \times Q)$ depicts matrix size, further K denotes the Haar transform while $(Q \times Q)$ depicts the size, that includes the Haar functions which have been described in the interval $Z \in 0, 1$ for $a = 0, 1 \dots \dots \dots Q-1$ as well as $Q = 2^p$. For producing the S, a can be illustrated by:

$$1 = 2^c + e - 1;\ 0 \le c \le p-1;\ c = 0\ ;\ 1 \le c \le 2^c\ ;\ c \ne 0 \quad \dots (2)$$

Haar basis functions have been explained well. While imposing Haar wavelet transform to a source image A_j with dimension $(Q \times Q)$, here samples are visualized as single row respective to the source image and filtered by filters low-pass and high pass filters; further down sampling of the produced output is done to generate the sub-coefficients L as well H images, denoting respectively low frequency as well as high frequency images. Further both of the images are filtered involving low pass and high pass filters as well as down sampling is done for generating the sub coefficients LL, HL, LH as well as HH, which are further fused via proposed fusion scheme to gain the fused image of same dimension $(Q \times Q)$. Here low frequency sub-coefficients are denoted through LL while high frequency sub-coefficients are denoted through HL, LH as well HH. These aforementioned frequency sub-coefficients are utilized for medical imaging where images are amalgamated with complementary information details for preserving sensitive information/details for facilitating diagnosis. Here two medical image modalities extracted out of the BRATS image database denoted via $W_1(a,b)\ and\ W_2(a,b)$ involves low pass as well as high pass filters for generation of low frequency subgroups and high frequency subgroups illustrated as following:

$$W_1^L(a,b) = \sum_{u=-E}^{E}\sum_{V=-E}^{E}[W_1(a,b) \times L(a-u)(b-v)] \quad \dots (3)$$

$$W_1^H(a,b) = \sum_{u=-E}^{E}\sum_{V=-E}^{E}[W_1(a,b) \times H(a-u)(b-v)] \quad \dots (4)$$

The low- as well as high-frequency coefficients $W_1^L(a,b)$ and $W_1^H(a,b)$ have been generated by convolution of source images by utilizing filter function, where $*$ points out convolutional operator as well as E denotes the presence of total pixels in the image. In a similar way four sub-coefficients such as HH, LH, HL and LL have been produced via imposing three high pass filters in horizontal, vertical as well as diagonal directions and one low pass filter. In similar fashion further one low pass as well as three high pass filters in horizontal, vertical as well as diagonal directions are imposed along the columns in $W_1^L\ (a,b)$ to generate the four image subparts denoted via LL, HL, LH as well as HH to obtain the subbands

$$W_1^{HH}(a,b), W_1^{LH}(a,b), W_1^{HL}(a,b)\ and\ W_1^{LL}(a,b)$$

Moreover while applying the low pass and high pass filters to the second input image $W_2(a,b)$, we may describe mathematically as the following:

$$W_2^L(a,b) = \sum_{u=-E}^{E}\sum_{V=-E}^{E}[W_2(a,b) \times L(a-u)(b-v)] \quad \dots (5)$$

$$W_2^H(a,b) = \sum_{u=-E}^{E}\sum_{V=-E}^{E}[W_2(a,b) \times H(a-u)(b-v)] \quad \ldots (6)$$

The sub-parts of images are obtained via imposing filters (low as well as high pass filters). Three directions involves horizontal, vertical as well as diagonal for imposing filter. Further image subparts are obtained as $W_2^{LL}(a,b), W_2^{LH}(a,b), W_2^{HL}(a,b)$ *and* $W_2^{HH}(a,b)$. The input images $W_1(a,b)$ and $W_2(a,b)$ further will be segregated into sub-images represented as:

$$W_1^{LL}(a,b) = \sum_{u=-E}^{E}\sum_{V=-E}^{E}[W_1^L(a,b) \times L(a-u)(b-v)] \quad \ldots (7)$$

$$W_2^{LL}(a,b) = \sum_{u=-E}^{E}\sum_{V=-E}^{E}[W_2^L(a,b) \times L(a-u)(b-v)] \quad \ldots (8)$$

$$W_1^{HH}(a,b) = \sum_{u=-E}^{E}\sum_{V=-E}^{E}[W_1^H(a,b) \times H(a-u)(b-v)] \quad \ldots (9)$$

$$W_2^{HH}(a,b) = \sum_{u=-E}^{E}\sum_{V=-E}^{E}[W_2^H(a,b) \times H(a-u)(b-v)] \quad \ldots (10)$$

$$W_1^{HL}(a,b) = \sum_{u=-E}^{E}\sum_{V=-E}^{E}[W_1^H(a,b) \times L(a-u)(b-v)] \quad \ldots (11)$$

$$W_2^{HL}(a,b) = \sum_{u=-E}^{E}\sum_{V=-E}^{E}[W_2^H(a,b) \times L(a-u)(b-v)] \quad \ldots (12)$$

$$W_1^{LH}(a,b) = \sum_{u=-E}^{E}\sum_{V=-E}^{E}[W_1^L(a,b) \times H(a-u)(b-v)] \quad \ldots (13)$$

$$W_2^{LH}(a,b) = \sum_{u=-E}^{E}\sum_{V=-E}^{E}[W_2^L(a,b) \times H(a-u)(b-v)] \quad \ldots (14)$$

The above mentioned image sub-coefficients demonstrate that the sub-pictures are framed with the two-level decomposition technique. The sub-pictures extricated utilizing the Haar wavelet transforms are utilized for fusion of multi-modal images utilizing proposed fusion strategy. Here, Haar wavelet transform is applied on both MRI images E and F. Here, the wavelets are sampled in a discrete manner. The goal is that it poses over block assisted transforms in which it capture both spatial and frequency information. The Haar transform is obtained from the Haar matrix.

The Haar transform is considered as sampling procedure wherein the transformation matrix rows are considered as samples of better resolution. The main function of Haar wavelet while adapted to 2D discrete signal contains $N \times N$ samples wherein every image row are filtered using high-pass, low-pass filter as well as resultant product is down-sampled with two to generate transient images L, H. Here, the L refers original image which is low-pass filtered as well as down-sampled in x-direction.

Here, the four sub-band images are integrated for creating an output image using similar count of samples as original. Here, the LL refers: original image, HL signifies: in vertical direction and high-pass filtered, LH represents: in horizontal direction and high-pass filtered, moreover HH signifies: in horizontal and vertical directions and is high-pass filtered. The four sub-band images involve all the information present in input image. Haar wavelet transform applying to source images is T_1 as well as T_2.

Correlation-weighted Fusion Model

The correlation-based weighted fusion model is utilized to fuse obtained Haar wavelet transform of T_1 and T_2, in order to attain the fused medical image. Correlation is a measure that computes the degree to which the two attributes move in relation to each other. Here, the combination of T_1 and T_2 is performed with correlation, and is given by,

$$G = \alpha T_1 + (1-\alpha)T_2 \quad \ldots (15)$$

where, α refers correlation amongst T_1 and T_2, Haar wavelet of MRI image-1 is denoted by T_1 and Haar wavelet of MRI image-2 is denoted by T_2.

Fusion Using Proposed Adaptive Taylor ASSCA-DCNN

The fused output G is considered as an input to Deep CNN. Deep CNN training is performed with devised Adaptive Taylor ASO + SCA. The final fusion is done for augmenting the contrast of fused image. Here, the fusion is performed with Deep CNN wherein optimum fusion score is chosen with Adaptive Taylor ASO + SCA, which is generated by integrating adaptive concept in Taylor ASO + SCA.

Architecture of Deep Convolutional Neural Network

The Deep CNN structure[28] consist of three layers, such as Fully Connected (FC), convolutional i.e. conv as well as pooling i.e. POOL layers in which every layer adapts separate functions. Here, FC layer is liable to perform fusion process. The structure of Deep CNN is depicted in Fig. 2.

-*Conv layers:* Here, conv layer mines imperative information contained in the image, and is expressed by,

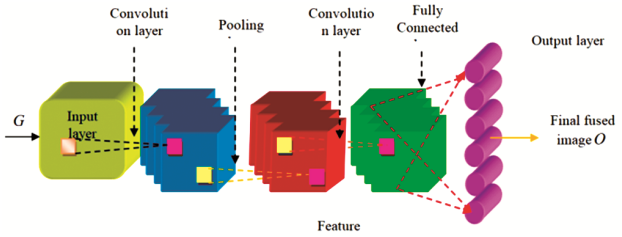

Fig. 2 — Structure of Deep CNN

$$B = \{B_1, B_2, \ldots, B_e, \ldots, B_f\} \quad \ldots (16)$$

where, f symbolizes total conv layers, and e^{th} conv layer is represented by B_e. The units located in $(j\,k)$ acquires output, and is illustrated as,

$$\left(B_\sigma^b\right)_{j,k} = \left(\varepsilon_\sigma^b\right)_{j,k} + \sum_{y=1}^{Y_1^{j-1}} \sum_{r=-h_1^\sigma}^{h_1^\sigma} \sum_{v=-h_2^\sigma}^{h_2^\sigma} \left(M_{b,y}^\sigma\right)_{r,v} * \left(B_\sigma^{b-1}\right)_{j+z,k+v} \quad \ldots (17)$$

where, $*$ express conv operator, $\left(B_\sigma^b\right)_{j,k}$ refers static feature maps out of convolution layer σ, while Y_1^{j-1} signifies overall feature maps, whereas $\left(M_{b,y}^\sigma\right)_{r,v}$ symbolize weights, and is training is accompanied via proposed Adaptive Taylor ASO + SCA algorithm, ε_σ^b symbolize bias of σ^{th} convolution layer, $\left(B_\sigma^{b-1}\right)_{j+z,k+v}$ refers feature map of prior convolution layer, whereas $M_{b,y}^\sigma$ signifies kernel function.

-ReLU: For accelerating the highest efficiency ReLU has signified an activation module. The result produced with ReLU layer may be demonstrated via equation (18),

$$B_y^b = fun\left(B_y^{b-1}\right) \quad \ldots (18)$$

where, $fun(\,)$ represents y^{th} layer pertaining activation function.

-FC layers: Here patterns were obtained via convolutional and pooling layers further inputting as an input for fully connected layers for performing multimodal image amalgamation. Final produced outcome generated with FC is given by, $V_\sigma^b = W\left(a_\sigma^b\right)$ with

$$a_\sigma^b = \sum_{y=1}^{Y_1^{\sigma-1}} \sum_{r=-h_1^\sigma}^{h_1^\sigma} \sum_{v=-h_2^\sigma}^{h_2^\sigma} \left(M_{b,y}^\sigma\right)_{r,v} * \left(B_\sigma^{b-1}\right)_{l+z,m+v} \quad \ldots (19)$$

where, $\left(M_{b,y}^\sigma\right)_{r,v}$ symbolize weight associating (j,k) in r^{th} feature map of layer $\sigma-1$ and s^{th} unit in layer σ. The output generated from Deep CNN is given by O, and is trained with proposed Adaptive Taylor ASO + SCA.

Training of Deep CNN using proposed Adaptive Taylor ASO + SCA

Here DCNN is trained via proposed Adaptive Taylor ASO + SCA, which is developed by combining adaptive concept in Taylor ASO + SCA. The Taylor ASO + SCA describe the complex variables, which are extension of function into infinite terms. It helps to compute integrals as well as infinite sums through discovering the Taylor series. It contains the capability to manage high-order terms. It provides improved trade off amongst the exploration and exploitation. In adaptive theory, the adaptive constants adjust the control attributes without user interface. Hence, the combination of adaptive concept in Taylor ASO + SCA offers enhanced convergence to generate global optimal solutions. Thus, the incorporation of adaptive concept in Taylor ASO + SCA assists to enhance overall performance. The steps of proposed Adaptive Taylor ASO + SCA is expressed as,

Step 1) Initiation: In initial step solutions are initialized, which may be illustrated as, J with total λ solution, here $1 \le \mu \le \lambda$

$$J = \{J_1, J_2, \ldots, J_\mu, \ldots, J_\lambda\} \quad \ldots (20)$$

Here, J_μ depicts the μ^{th} solution , λ represents total solution, moreover $J \in \omega, \beta$ as J belongs to weight as well as bias.

Step 2) Determination of Error: Error function helps in determining the optimum solution, and is considered like minimization issue as well as depicted as follows,

$$\mathrm{MS}_{\mathrm{err}} = \frac{1}{\mathrm{g}} \sum_{\mathrm{h}=1}^{\mathrm{g}} \left[\mathrm{K_h} - \mathrm{O}\right]^2 \quad \ldots (21)$$

where, K_h symbolize expected output, and O express output obtained from Deep CNN, g refers count of data, for example; $1 < h \le g$.

Step 3) Update Equation Discovery: The update of Adaptive Taylor ASO + SCA is given by,

$$J_c(m+1) = \left[1 - \frac{2s_1s_3\mathrm{Sin}(s_2)d_c(m)}{s_1s_3\mathrm{Sin}(s_2)d_c(m) - \eta e^{\frac{-20m}{M}}}\left(1 - \eta e^{\frac{-20m}{M}}\left(\frac{1 - s_1\mathrm{Sin}(s_2) + s_1s_3\mathrm{Sin}(s_2)}{s_1s_3\mathrm{Sin}(s_2)d_c(m)}\right)\right)\right]^{-1} \frac{s_1s_3\mathrm{Sin}(s_2)d_c(m)}{s_1s_3\mathrm{Sin}(s_2)d_c(m) - \eta e^{\frac{-20m}{M}}}$$
$$\left[2\left[\begin{array}{c}1.359J_c(m-2) - 1.3591J_c(m-1) - 0.6795J_c(m-3)\\ +0.2259J_c(m-4) - 0.0555J_c(m-5) + 0.0104J_c(m-6) - 1.38e^{-3}J_c(m-7) + 9.92e^{-5}J_c(m-8)\end{array}\right] - Y + Rand_c a_c(m)\right] \quad \ldots (22)$$

where, s_1 indicate movement direction, s_2 determines at what distance advancement should be towards target, s_3 offers random target weight, $Rand_a(m)$ symbolize arbitrary number in $[0,1]$ in current iteration, η indicate multiplier weight, $d_c(m)$, the depth weight, and $Sin(s_2)$ express sine component, $J_c(m-x)$ represent Taylor series such that $x=1,2,\ldots,8$.

Here,

$$Y=\beta\left(1-\frac{m-1}{M}\right)^3 e^{\frac{-20m}{M}} \sum_{f\in A_{BEST}} \frac{Rand_f\left[2\times\left(l_{cf}(m)\right)^{13}-l_{cf}^7\right]}{p_a(b)} \frac{J_f(m)-J_c(m)}{\|J_f(m),J_c(m)\|_2},$$

such that velocity is expressed as $J_f(m)$, depth weight is expressed as β, and mass is represented as $p_a(b)$.

In proposed Adaptive-Taylor ASO + SCA the update is performed using Taylor ASO+SCA algorithm by making the constants self adaptive. The random numbers s_1, s_2, s_3 are made self-adaptive. Consider $s=s_1,s_2,s_3$ wherein the s is made self-adaptive by formulating it as,

$$s=s_0\left[1-\beta\times\frac{m}{m_{\max}}\right] \quad \ldots (23)$$

where, s_0 is constant, β represent scaling factor, and $m_{\max}$ is maximum iteration.

Step 4) Re-assess error for update solutions: The error update solutions are re-examined where best solution is gained for energy forecast.

Step 5) Termination: Here optimum solutions are devised in iterative way till highest iterations are acquired.

Results and Discussion

The efficiency of proposed Adaptive Taylor ASO + SCA-based Deep CNN using MI, RMSE and PSNR is deliberated.

Experimental Setup

The designed model is implemented in MATLAB tool utilizing Windows 10 Operating System, core processor of Intel I3 and RAM of 2GB using BRATS 2018 dataset. The assessment of methods is done utilizing BRATS 2018 dataset[29] consisting of MRIs and segmentation of brain tumour with ground truth samples considering 4 MRI modalities like T1, T1c, T2 as well as FLAIR. In addition, the medical image modalities are obtained with 19 institutions considering distinct MRI.

Key Performance Indicators

Here efficiency of proposed Adaptive Taylor ASO + SCA-based Deep CNN is analyzed with several efficiency measures using the MI, RMSE and PSNR.

a) MI: MI is used for assessing how much mutual dependence exists in two pictures, and can be outlined in following way:

$$U=\frac{1}{2}\left[R\left[H(j,z),O(j,z)\right]MI\left[P(j,z),O(j,z)\right]\right] \ldots (24)$$

where, $H(j,z)$ and $P(j,z)$ indicates two input, and fused image is expressed as $O(j,z)$.

b) RMSE: Use of RMSE is done to calculate the error generated via fused model, mathematically expressed as:

$$M=\frac{1}{2}\left[M\left[H(j,z),O(j,z)\right]+M\left[P(j,z),O(j,z)\right]\right] \ldots (25)$$

c) PSNR: It indicates ratio of highest possible signal power to affected noise. Here unit of measuring PSNR is decibel (dB) where it may be denoted in following mathematical form,

$$PSNR=10\log_{10}\left(\frac{R_{\max}{}^2}{MSE}\right) \quad \ldots (26)$$

where, $R_{\max}$ expresses pixel's peak value, and MSE expresses mean square error.

Experimental Results

Experimental outcomes of proposed work via Adaptive Taylor ASSCA-based Deep CNN using set of inputted MRI images enlisted in Fig. 3. In all four rows, the input MRI image-1, image-2 and fused image are displayed as (a), (b) and (c) respectively.

Comparative Techniques and Analytical Demonstration

The proposed Adaptive Taylor ASSCA−Deep CNN is compared with like Discrete Wavelet Transform (DWT) + Holoentropy Whale fusion (HWFusion) + SP − Whale[30], DWT+ undecimated DWT (UDWT) + Genetic Algorithm (GA)[31], DWT+ASO + SCA + Renyi entropy[32], ASO + SCA-based Deep CNN[33] as well as DTCWT-based weighted fusion.[34]

The efficiency of developed Adaptive Taylor ASO + SCA-based Deep CNN is computed using MI, RMSE and PSNR with BRATS 2018 database.

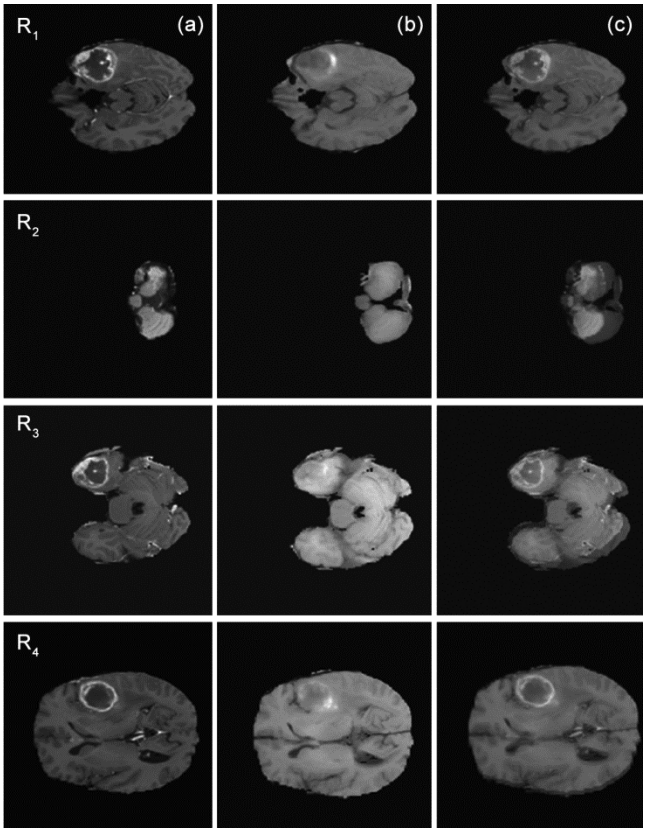

Fig. 3 — Experimental outcomes of proposed scheme (all four rows): (a) Source image-1, (b) Source image-2, (c) Fused image

***a)* Assessment with Sym2**

The assessment with sym 2 (symlet) has been shown in Fig. 4. The assessment with MI, PSNR, RMSE is displayed in Fig. 4 (a), (b), (c) respectively.

b) Assessment with Db2

The assessment with db 2 (Daubechies) is illustrated in Fig. 5. The assessment using MI, PSNR, RMSE have been shown in Fig. 5 (a), (b) & (c) respectively.

Comparative Assessment Description

We have included simulation assessments with MI, PSNR and RMSE in Table 1. Using sym 2 and db 2 for 5 image pairs taken from the BRATS dataset, here our proposed fusion scheme is delivering better performance for all of the key indicators listed in the experimental Table 1. The highest MI of 1.672532 have been depicted using db 2 wavelet for image pair1, highest PSNR 42.20993 using db 2 wavelet for image pair 5 and lowest RMSE 5.204896 using sym 2 wavelet for image pair 5, have been shown for our proposed fusion scheme named as Adaptive Taylor ASO + SCA-based Deep CNN. The proposed

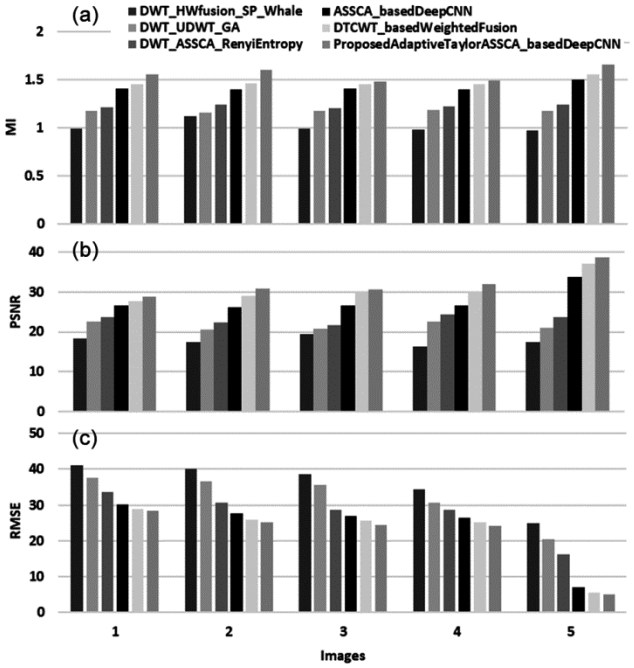

Fig. 4 — Assessment with sym2: (a) MI, (b) PSNR, (c) RMSE

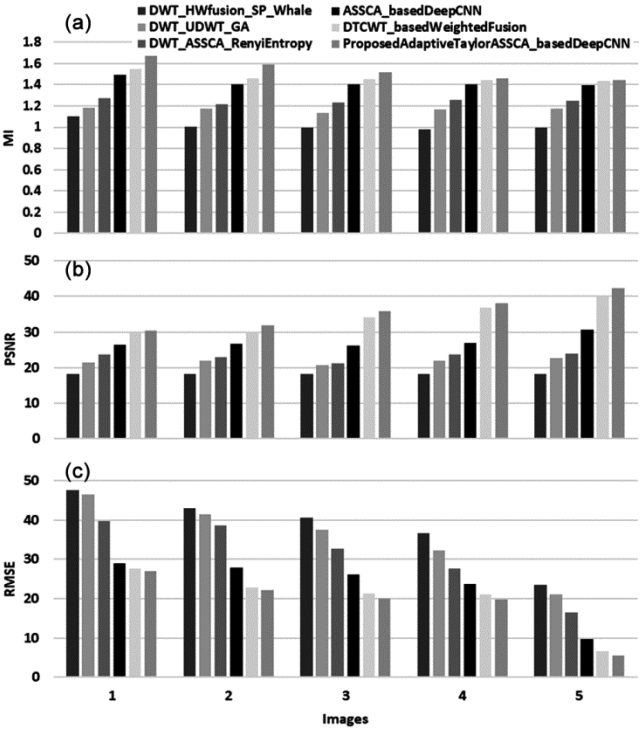

Fig. 5 — Assessment with db2: (a) MI, (b) PSNR, (c) RMSE

Adaptive Taylor ASO + SCA-based Deep CNN attained high mutual information, which indicates that there is large reduction in uncertainty. The highest PSNR of 42.20993 dB is evaluated by proposed Adaptive Taylor ASO + SCA-based Deep CNN. The highest PSNR ensures that the proposed Adaptive

Table 1 — Analysis Using db2 and Sym2 Wavelet (For Images 1 to 5)

Images	Wavelet	Metrics	Ref.[30]	Ref.[31]	Ref.[32]	Ref.[33]	Ref.[34]	Proposed
1	db2	RMSE	47.59881	46.5924	39.60645	29.08496	27.73134	26.96568
2	db2	RMSE	43.09881	41.5124	38.60651	27.90118	22.87109	22.18417
3	db2	RMSE	40.59881	37.5724	32.60481	26.15327	21.28333	19.92036
4	db2	RMSE	36.59881	32.2624	27.60651	23.76265	21.10935	19.83597
5	db2	RMSE	23.59881	21.1624	16.60621	9.74028	6.598654	**5.661937**
1	db2	MI	1.0982	1.180084	1.271816	1.491514	1.54924	**1.672532**
2	db2	MI	1.004	1.175433	1.216521	1.403362	1.456722	1.586727
3	db2	MI	0.992411	1.130233	1.229313	1.399082	1.453211	1.514929
4	db2	MI	0.97621	1.167608	1.255187	1.39926	1.440918	1.460242
5	db2	MI	0.992411	1.17497	1.251461	1.398326	1.432985	1.447027
1	db2	PSNR(dB)	18.28749	21.5469	23.6348	26.4013	29.81349	30.35271
2	db2	PSNR(dB)	18.28749	22.00938	23.01742	26.61908	30.1987	31.87736
3	db2	PSNR(dB)	18.28749	20.72529	21.33843	26.25751	34.01838	35.90222
4	db2	PSNR(dB)	18.28749	22.01543	23.66897	26.95131	36.87254	38.11101
5	db2	PSNR(dB)	18.28749	22.66027	23.8643	30.60136	40.45891	**42.20993**
1	Sym2	RMSE	41.15944	37.53765	33.56301	30.10118	28.97987	28.35383
2	Sym2	RMSE	40.15944	36.53602	30.56301	27.6506	25.95205	25.13857
3	Sym2	RMSE	38.48785	35.53556	28.56301	26.84027	25.61862	24.55959
4	Sym2	RMSE	34.40144	30.5376	28.56301	26.34023	25.30825	24.09777
5	Sym2	RMSE	24.90144	20.53665	16.1563	7.058641	5.554428	**5.204896**
1	Sym2	MI	0.992411	1.172494	1.206321	1.402086	1.446218	1.555663
2	Sym2	MI	1.121135	1.150434	1.236033	1.398918	1.457243	1.601893
3	Sym2	MI	0.992411	1.172494	1.196321	1.402086	1.446218	1.475335
4	Sym2	MI	0.982411	1.181018	1.21716	1.398554	1.447609	1.487299
5	Sym2	MI	0.972411	1.175823	1.234643	1.500041	1.554532	**1.653671**
1	Sym2	PSNR(dB)	18.36369	22.60148	23.59412	26.58635	27.67342	28.71412
2	Sym2	PSNR(dB)	17.4578	20.61496	22.28488	26.22666	28.97654	30.7199
3	Sym2	PSNR(dB)	19.36369	20.75698	21.63724	26.66911	29.83722	30.65913
4	Sym2	PSNR(dB)	16.36369	22.4781	24.38034	26.62927	30.17383	31.86039
5	Sym2	PSNR(dB)	17.36369	20.98028	23.64028	33.6511	37.03477	**38.5168**

Taylor ASO + SCA-based Deep CNN effectively fused the multimodal medical images without compromising the quality. The smallest RMSE of 5.204896 is measured by proposed Adaptive Taylor ASO + SCA-based Deep CNN. The smallest RMSE ensures that this method is not susceptible to any kind of error and there is no good or bad threshold that could degrade performance. The highest MI of 1.672532 have been depicted using db2 wavelet for image pair1, highest PSNR 42.20993 dB using db 2 wavelet for image pair 5 and lowest RMSE 5.204896 using sym 2 wavelet for image pair 5, have been shown via proposed Adaptive Taylor ASO + SCA-based Deep CNN. Through experimental results and examination our proposed strategy displayed for protecting edge as well as component related data, additionally tumour identification effectiveness has likewise been expanded.

Conclusions

An adaptive optimization driven deep model is developed for multimodal medical image fusion using MRI images. The proposed Adaptive Taylor ASO + SCA-Deep CNN effectively performed multimodal medical image fusion using set of MRI images. The proposed Adaptive Taylor ASO + SCA-Deep CNN provided enhanced performance with the highest MI of 1.672532, highest PSNR 42.20993dB and lowest RMSE 5.204896, have been shown via proposed Adaptive Taylor ASO + SCA-based Deep CNN. Thus, the proposed technique has showed improved efficiency in contrast to other methods based on fusion performance and visual quality. Through experimental outcomes it is effectively inferred that our proposed strategy displayed for protecting edge as well as component related data, additionally tumour identification effectiveness has likewise been

enhanced. In addition to ensuring the amalgamation of multimodality images for enhancement of the single modality image for making the merged image useful for making medical decisions, the proposed model also produces high-quality images. The wavelets are created by deriving them out of the input images utilizing the Haar wavelet transform, that helps with pixel-wise fusion and produces important image information. Here the highest mutual information, which indicates that there is large reduction in uncertainty. Here the highest PSNR ensures that the proposed Adaptive Taylor ASO + SCA-based Deep CNN effectively fused the multimodal medical images without compromising the quality. The smallest RMSE ensures that this method is not susceptible to any kind of error and there is no good or bad threshold that could degrade performance. In future, other hybrid optimization algorithms can be utilized to produce more significant results for clinical diagnosis through clinical imaging.

Abbreviations used

Deep CNN	Deep convolution neural network
ASO	Atom search optimization
ASSCA	Atom search sine cosine algorithm
DWT	Discrete wavelet transform
UDWT	Undecimated discrete wavelet transform
GA	Genetic algorithm
Db2	Daubechies 2 wavelet
Sym2	Symlets 2 wavelet
DTCWT	Dual tree complex wavelet transform
MRI	Magnetic resonance imaging
SCA	Sine cosine algorithm
SPECT	Single-photon emission computerized tomography (scan image)
PET	Positron emission tomography (scan image)

References

1 Kaur M & Singh D, Multi–modality medical image fusion technique using multi-objective differential evolution based deep neural networks, *J Ambient Intell Hum Comput*, **12(2)** (2021) 2483–2493.

2 Dinh P H, Multi-modal medical image fusion based on equilibrium optimizer algorithm and local energy functions, *Appl Intell*, **51(21)** (2021) 1–16.

3 Li Y, Zhao J, Lv Z & Li J, Medical image fusion method by deep learning, *Int J Cognit Comput Eng*, **2** (2021) 21–29.

4 Huang X, Zhang B, Zhang X, Tang M, Miao Q, Li T & Jia G, Application of U-Net based multiparameter magnetic resonance image fusion in the diagnosis of prostate cancer, *IEEE Access*, **9** (2021) 33756–33768.

5 Khan U, Paheding S, Elkin C & Devabhaktuni V, Trends in deep learning for medical hyperspectral image analysis, *IEEE Access*, **9** (2021) 79534–79548.

6 Kong W, Li C & Lei Y, Multimodal medical image fusion using convolutional neural network and extreme learning machine, *Front Neurorob*, (2022).

7 Kumar V, Gupta A, Hazarika B B & Gupta D, Automatic diagnosis of COVID-19 from Chest X-ray images using transfer learning-based deep features and machine learning models (2022).

8 Zhou T, Li Q, Lu H, Cheng Q & Zhang X, GAN review: Models and medical image fusion applications, *Information Fusion*, **91** (2023) 134–148.

9 Singh V & Kaushik V D, HoEnTOA: Holoentropy and Taylor assisted optimization based a novel image quality enhancement algorithm for multi-focus image fusion, *J Sci Ind Res*, **80(10)** (2021) 875–886, Doi: 10.56042/jsir.v80i10.52244

10 [10] Guo P, Xie G, Li R & Hu H, Multimodal medical image fusion with convolution sparse representation and mutual information correlation in NSST domain, *Complex & Intelligent Systems*, **9(1)** (2023) 317–328.

11 Srikanth M V, Prasad V V K D V & Prasad K S, Brain tumor detection through modified optimization algorithm by region-based image fusion, *ECTI Trans Comput Inf Technol*, **17(1)** (2023) 117–127.

12 Singh V & Kaushik V D, A study of multi-focus image fusion: State-of-the-art techniques, in *Advances in Data and Information Sciences: Proceedings of ICDIS 2021* (Springer Singapore) 2022, 563–572, Doi: 10.1007/978-981-16-5689-7_49.

13 Singh V & Kaushik V D, A Typical Hybrid Optimization-Based Image Quality Enhancement Technique, in *Proceedings of International Conference on Computational Intelligence, Data Science and Cloud Computing: IEM-ICDC 2021* (Springer Nature Singapore) 2022, 225-233, Doi: 10.1007/978-981-19-1657-1_18.

14 [14] Singh V & Kaushik V D, A Brief Study and Overview of Image Fusion Methods, In *Proceedings of International Conference on Computational Intelligence, Data Science and Cloud Computing: IEM-ICDC 2020*, *Springer Singapore*, (2021) 355–367, Doi: 10.1007/978-981-33-4968-1_28.

15 Azam M A, Khan K B, Salahuddin S, Rehman E, Khan S A, Khan M A & Gandomi A H (2022). A review on multimodal medical image fusion: Compendious analysis of medical modalities, multimodal databases, fusion techniques and quality metrics, *Comput Biol Med*, **144** (2022) 105253.

16 Pei C, Fan K & Wang W, Two-scale multimodal medical image fusion based on guided filtering and sparse representation, *IEEE Access*, **8** (2020) 140216–140233.

17 Nejati M, Samavi S, Karimi N, Soroushmehr S R, Shirani S, Roosta I & Najarian, Surface area-based focus criterion for multi-focus image fusion, *Inf Fusion*, **36** (2017) 284–295.

18 Jin X, Chen G, Hou J, Jiang Q, Zhou D & Yao S, Multimodal sensor medical image fusion based on nonsubsampled shearlet transform and S-PCNNs in HSV space, *Signal Process*, **153** (2018) 379–395.

19 Yang Y, Tong S, Huang S & Lin P, Log-Gabor energy based multimodal medical image fusion in NSCT domain, *Comput Math Methods Med* (2014).

20 Irshad M T & Rehman H U, Gradient compass-based adaptive multimodal medical image fusion, *IEEE Access*, **9** (2021) 22662–22670.

21 Jose J, Gautam N, Tiwari M, Tiwari T, Suresh A, Sundararaj V & Rejeesh M R, An image quality enhancement scheme employing adolescent identity search algorithm in the NSST

domain for multimodal medical image fusion, *Biomed Signal Process Control*, **66** (2021) 102480.
22 Shehanaz S, Daniel E, Guntur S R & Satrasupalli S, Optimum weighted multimodal medical image fusion using particle swarm optimization, *Optik*, **231** (2021) 166413.
23 Li X, Zhou F, Tan H, Zhang W & Zhao C, Multimodal medical image fusion based on joint bilateral filter and local gradient energy, *Inf Sci*, **569** (2021) 302–325.
24 He C, Liu Q, Li H & Wang H, Multimodal medical image fusion based on IHS and PCA, *Procedia Eng,* **7** (2010) 280–285.
25 Bhatnagar G, Wu Q J & Liu Z, Directive contrast based multimodal medical image fusion in NSCT domain, *IEEE Trans Multimedia*, **15(5)** (2013) 1014–1024.
26 Huang B, Yang F, Yin M, Mo X & Zhong C, A review of multimodal medical image fusion techniques, *Comput Math Methods Med* (2020).
27 Tedmori S & Al-Najdawi N, Image cryptographic algorithm based on the Haar wavelet transform, *Inform Sci*, **269** (2014) 21–34.
28 Tu F, Yin S, Ouyang P, Tang S, Liu L & Wei S, Deep convolutional neural network architecture with reconfigurable computation patterns, *IEEE Trans Very Large Scale Integr VLSI Syst*, **25(8)** (2017) 2220–2233.
29 Multimodal Brain Tumor Segmentation Challenge 2018 (BraTS), [https://wiki.cancerimagingarchive.net/pages/viewpage.action?pageId=37224922" accessed on July 2021].
30 Venkatrao P H & Damodar SS, HWFusion: Holoentropy and SP-Whale optimisation-based fusion model for magnetic resonance imaging multimodal image fusion, *IET Image Process*, **12(4)** (2018) 572–581.
31 Kavitha S & Thyagharajan K K, Efficient DWT– based fusion techniques using genetic algorithm for optimal parameter estimation, *Soft Comput*, **21(12)** (2017) 3307–3316.
32 Singh V & Kaushik V D, Renyi entropy and atom search sine cosine algorithm for multi focus image fusion, *Signal Image Video Process*, **15** (2021) 903–912, Doi: https://doi.org/10.1007/s11760-020-01814-0.
33 Singh V and Kaushik V D, WeAbDeepCNN: Weighted average model and ASSCA based two level fusion scheme for multi-focus Images, *J Sci Ind Res*, **80(10)** (2021) 905–914, Doi: 10.56042/jsir.v80i10.46870.
34 Singh, V & Kaushik, V D, DTCWTASODCNN: DTCWT based weighted fusion model for multimodal medical image quality improvement with ASO technique & DCNN, *J Sci Ind Res*, **81(08)** (2022) 850–858, Doi: 10.56042/jsir.v81i08.56203.